Some Aspects of Forecasting Severe Thunderstorms during Cool-Season Return-Flow Episodes

STEVEN J. WEISS

NOAA National Weather Service, National Severe Storms Forecast Center, Kansas City, Missouri

(Manuscript received 12 April 1991, in final form 20 November 1991)

ABSTRACT

Historically, the Gulf of Mexico has been considered a primary source of water vapor that influences the weather for much of the United States east of the Rocky Mountains. Although severe thunderstorms and tornadoes occur most frequently during the spring and summer months, the periodic transport of Gulf moisture inland ahead of traveling baroclinic waves can result in significant severe-weather episodes during the cool season.

To gain insight into the short-range skill in forecasting surface synoptic patterns associated with moisture return from the Gulf, operational numerical weather prediction models from the National Meteorological Center were examined. Sea level pressure fields from the Limited-Area Fine-Mesh Model (LFM), Nested Grid Model (NGM), and the aviation (AVN) run of the Global Spectral Model, valid 48 h after initial data time, were evaluated for three cool-season cases that preceded severe local storm outbreaks. The NGM and AVN provided useful guidance in forecasting the onset of return flow along the Gulf coast. There was a slight tendency for these models to be slightly slow in the development of return flow. In contrast, the LFM typically overforecasts the occurrence of return flow and tends to "open the Gulf" from west to east too quickly.

Although the low-level synoptic pattern may be forecast correctly, the overall prediction process is hampered by a data void over the Gulf. It is hypothesized that when the return-flow moisture is located over the Gulf, model forecasts of stability and the resultant operational severe local storm forecasts are less skillful compared to situations when the moisture has spread inland already. This hypothesis is tested by examining the performance of the initial second-day (day 2) severe thunderstorm outlook issued by the National Severe Storms Forecast Center during the Gulf of Mexico Experiment (GUFMEX) in early 1988.

It has been found that characteristically different air masses were present along the Gulf coast prior to the issuance of outlooks that accurately predicted the occurrence of severe thunderstorms versus outlooks that did not verify well. Unstable air masses with ample low-level moisture were in place along the coast prior to the issuance of the "good" day 2 outlooks, whereas relatively dry, stable air masses were present before the issuance of "false-alarm" outlooks. In the latter cases, large errors in the NGM 48-h lifted-index predictions were located north of the Gulf coast.

1. Introduction

The Gulf of Mexico has long been thought to be the primary source of water vapor for general precipitation and severe thunderstorm development over much of the United States east of the Rocky Mountains (e.g., Newton 1963). The influence of the Gulf as a source of moist air can be seen in a schematic model of synoptic features associated with severe convective storms over the south-central United States (Fig. 1). Djurić and Damiani (1980) and Djurić and Ladwig (1983) investigated the development of the low-level jet (LLJ) over the southern plains during the cool season and identified a sequence of synoptic stages that are associated with the return flow of moisture from the Gulf. This sequence includes the following: 1) an anticyclone moves eastward across the plains as a cold front enters the Gulf coast; 2) a dry southerly LLJ develops over the southern High Plains as the anticyclone moves east of the plains and a cyclogenesis occurs in the lee of the Rockies; 3) the southern part of the LLJ extends into the western Gulf and begins advecting moisture northward; 4) the cyclone intensifies and the LLJ advects additional moisture into the southern plains; and 5) the synoptic pattern evolves into one that is favorable for severe storms (as in Fig. 1) as the cyclone and LLJ continue to strengthen. Recently, Lanicci and Warner (1991a–c) documented the synoptic evolution associated with the return flow of Gulf moisture and the development of a specific thermodynamic environment favorable for spring severe thunderstorms. This evolution occurs when a relatively dry and stable air mass over the southern United States becomes increasingly moist and potentially unstable as a surface anticyclone moves toward the Atlantic coast and southerly flow develops over the southern plains. As detailed by Lan-

Corresponding author address: Steven J. Weiss, National Severe Storms Forecast Center, Room 1728, Federal Building, Kansas City, MO 64106.

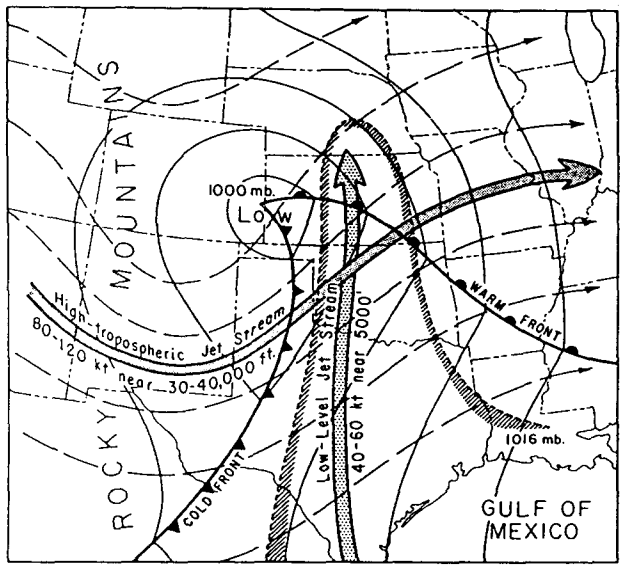

FIG. 1. Schematic model of synoptic features associated with a severe-weather outbreak over the south-central United States. Sea level isobars are solid, upper-tropospheric geopotential is dashed, and moist, potentially unstable air mass originating from the Gulf of Mexico is outlined by hatching (from Newton 1967).

icci and Warner (1991a), the airmass evolution involves the three-dimensional interaction of three airstreams such that 1) an approaching upper-level trough in the westerlies induces a southwesterly flow aloft of hot, dry air off the Mexican plateau; 2) this airstream moves over the southern plains and overruns a cooler, moister flow from the Gulf; and 3) a third airstream descends around the upper-level trough and forms a confluent–baroclinic zone along the west edge of the dry Mexican air. Since this evolution involves many complex kinematic and thermodynamic processes, the synoptic development of return flow is a difficult forecast problem during the winter and early spring. Furthermore, a wide variety of weather conditions may be associated with return-flow episodes, ranging from stratus, drizzle, and fog to severe thunderstorms and tornadoes.

The Gulf of Mexico Experiment (GUFMEX) was a multiagency limited field experiment organized by the National Severe Storms Laboratory (NSSL) to study 1) airmass modification over the Loop Current region when polar air moves southeastward over the Gulf and 2) characteristics of the return flow of modified polar air that subsequently returns northward into the southern plains and lower Mississippi Valley ahead of an approaching midlatitude cyclone. See Lewis et al. (1989) for an overview of GUFMEX.

The field phase of GUFMEX was conducted from 20 February through 2 April 1988 and utilized many data-gathering instruments to obtain meteorological and oceanographic information, including the National Oceanic and Atmospheric Administration (NOAA) P-3 aircraft, dropsondes, special National Weather Service (NWS) and Mexican Weather Service 6-h rawinsondes, and mobile sounding equipment from the National Center for Atmospheric Research. One airmass modification mission and five return-flow missions were conducted during the field phase. In all cases the 6-h upper-air observations surrounding the Gulf commenced 24 h before a flight mission day. Since preliminary notification to the upper-air stations was required 24 h prior to the release of the first special sounding, critical forecast decisions were made nearly 48 h before a GUFMEX field operations day. Accordingly, most decisions by the project forecast team were based upon guidance generated by operational numerical weather prediction models at the National Meteorological Center (NMC).

In order to incorporate NWS forecaster insight and experience into the forecasting portion of GUFMEX, project scientists routinely called upon regular duty forecasters at several NWS offices to assist in the decision-making process. This interaction between research meteorologists and NWS forecasters helped identify specific forecasting problems related to return-flow situations and also served to increase the spirit of cooperation and understanding between the research and operational sections. The GUFMEX forecast team consisted of operational forecasters in the NWS Southern Region and at the National Severe Storms Forecast Center (NSSFC) and research meteorologists from NSSL and the Cooperative Institute for Meteorological Satellite Studies (CIMSS) at the University of Wisconsin. The team was responsible for providing daily guidance and direction to support the data-gathering activities of the experiment and proved to be a successful combination of research and operational resources.

2. Use of numerical model guidance

Proper use of the numerical model guidance is dependent on an understanding of the performance characteristics of the different models in varying synoptic situations (e.g., Junker 1985; Junker et al. 1989; Caplan and White 1989). Of particular interest is the identification of any systematic errors exhibited by the models. Examinations of NMC model behavior have tended to focus on surface cyclone development (Leary 1971; Silberberg and Bosart 1982; Grumm and Siebers 1989a; Mullen and Smith 1990; Alexander and Young 1990) or midtropospheric circulation (Fawcett 1969; Hawes and Colucci 1986). Prior to the start of GUFMEX, however, several studies did examine surface anticyclone predictions from numerical models. Colucci and Bosart (1979) found that the 36-h prognoses from the six-layer primitive equation (6L-PE) model (Shuman and Hovermale 1968) underforecast the pressure and moved anticyclones too rapidly. More recently, Grumm and Gyakum (1986) examined the

48-h performance of the Limited-Area Fine-Mesh Model (LFM) (Gerrity 1977; Newell and Deaven 1981) and the Global Spectral Model (Sela 1980) during the 1980/81 cold season. They also found a tendency for both models to underforecast anticyclone pressure and to position anticyclones south and east of the observed positions.

Since the publication of these studies a new operational model, the Nested Grid Model (NGM: Phillips 1979; Hoke et al. 1989), has become the primary regional prediction model at NMC, and the spectral model has undergone significant upgrading in terms of resolution and model physics (Sela 1988; Kanamitsu 1989). Furthermore, little information was available concerning model performance in the forecasting of cold fronts into the Gulf and return-flow development, two topics that were of critical importance to GUFMEX. Therefore, a study was undertaken prior to the start of the field project to examine some relevant performance characteristics of the NMC models.

3. Synoptic cases and data sample

The period from November 1987 through January 1988 was examined to identify cases containing synoptic regimes similar to situations GUFMEX would study. It was recognized that this time period did not coincide with the GUFMEX operations window extending from mid-February into early April. However, substantive changes in the model structures of the NGM and AVN were made in 1987; these changes suggested that any model performance evaluation from previous years would be of questionable value. Although polar-air penetrations into the Gulf are typically more widespread and the development of return flow less frequent in the winter than the spring (Crisp and Lewis 1992), the synoptic characteristics of return-flow episodes in the winter are sufficiently similar to spring episodes (in terms of dynamic and thermodynamic factors) to justify studying model performance during the three months prior to GUFMEX.

In examining the surface synoptic patterns, the following generic scenario was identified: 1) a continental anticyclone moved east or southeast across the Great Plains and Mississippi Valley; 2) the anticyclone moved into the eastern states and a cold front marking the leading edge of polar air moved southeast across the Loop Current in the Gulf; and 3) the anticyclone moved toward the Atlantic coast and return flow over the northwest Gulf developed on the west side of the anticyclone. The return flow would be most meaningful if sufficient moisture was transported northward from the Gulf to contribute to important cool-season weather events. Although severe convective weather occurs most frequently during the spring and summer, nearly 10% of tornado outbreaks have been found to occur during the winter (Galway and Pearson 1981). Three episodes that satisfied these criteria during the period from November 1987 through January 1988 were associated with significant severe thunderstorm and tornado outbreaks over parts of the southern United States. The cases culminated in the following outbreaks:

1) the east Texas–lower Mississippi Valley outbreak of 15–16 November 1987;
2) the lower Mississippi Valley outbreak of 14 December 1987;
3) the lower Mississippi Valley–Tennessee Valley outbreak of 18–19 January 1988.

These outbreaks produced a total of 99 tornadoes, 52 large hail events, and 131 reports of thunderstorm wind damage, resulting in 22 deaths and 370 injuries. These cases are summarized in Figs. 2–4.

The 48-h forecasts of surface (mean sea level—MSL) pressure from the LFM, NGM, and the aviation (AVN) run of the spectral model preceding the severe local storm outbreaks were compiled. For each case, the start of the forecast evaluation began when the cold front was moving across the southern plains toward the Gulf, and ended when the return flow was well established and the Gulf was "open" for the return of moisture inland (see Table 1). All 48-h forecasts from the 0000 and 1200 UTC model runs for the 52 data periods were available except for two missing forecasts from the AVN.

The limited data sample raises several questions concerning the validity of the model evaluation results. First, the return-flow cases did not examine situations when severe storms failed to occur. Therefore, the applicability of the findings to all return-flow episodes has not been directly addressed. Operational forecasting experience, including predictions made during GUFMEX, suggests that surface patterns associated with return flow in severe-storm cases do not differ substantially from return flows that fail to produce severe storms. This observation is consistent with the results of Lanicci and Warner (1991a,c), who found that air masses with markedly different severe-storm potential were often associated with similar return-flow patterns in early spring. Therefore, it is believed that the model performance findings from this study should be useful in most return-flow situations. Second, the sample included successive model runs during similar synoptic patterns. It is possible that the "effective" sample size became smaller in a statistical sense because the error characteristics of successive model runs may be correlated (i.e., they are not independent). If similar errors are found on successive model runs, however, the results may reflect a systematic error that is meaningful to modelers and forecasters. It will be shown that the model anticyclone prediction errors are in good agreement with other studies that utilized more comprehensive databases (e.g., Grumm and Siebers 1989b). This suggests that the results are representative of typical model errors.

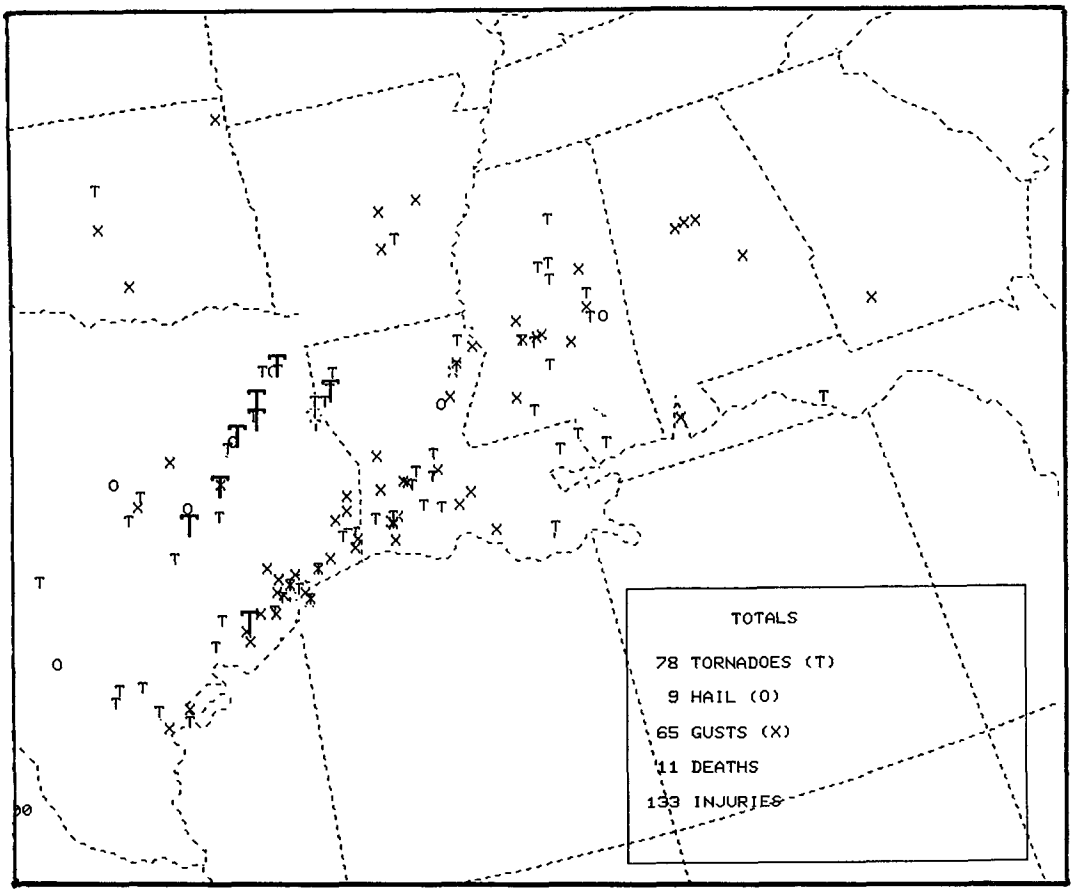

FIG. 2. Severe local storm events from 1200 UTC 15 November 1987 to 1200 UTC 17 November 1987. Killer tornadoes indicated by large "T."

4. Model predictions of return-flow kinematics

The model evaluations focused on the area of the Gulf of Mexico and the United States east of 105°W. Verifying conditions were obtained from the NGM 00-h forecast valid at the time of each 48-h forecast. The model forecasts and verifying conditions were examined for the following features: 1) location and intensity of primary surface anticyclones; 2) location of significant elongated ridge axes; 3) location of identifiable cold fronts moving into the Gulf; and 4) development of return flow over the western Gulf.

a. Prediction of surface anticyclone centers

In this study an anticyclone is defined as a point of high pressure surrounded by at least one closed isobar (4-mb interval) on the forecast or verifying charts. During the cool season anticyclones tend to be intense over continental areas, so the identification process was relatively straightforward. In most cases the evaluation involved the direct comparison between the labeled high pressure centers on the 48-h forecasts with the labeled centers on the verifying analyses.

In a few cases, however, the automated labels of the anticyclone centers on the NGM charts were more detailed than the LFM and AVN graphics. On these occasions a single primary anticyclone center was chosen, consisting of either 1) the actual highest pressure or 2) an interpolated center located equidistant between two adjacent labeled centers of equal pressure. This procedure was necessary; otherwise the more detailed structure of the NGM forecast and verifying analyses would likely bias the results in favor of the NGM. Finally, when an observed anticyclone center was not predicted, the accuracy of the forecast ridge axis was determined. This also was necessary to prevent any bias due solely to different labeling conventions of the different models and emphasized the importance of surface ridge location even when a labeled center was not present.

Central-pressure errors, displacement errors, and directional errors (eight-point compass) were tabulated for each anticyclone that was present on both the forecast and the verifying analyses. It can be argued that directional errors are of minimal importance when the forecast location is very close to the observed location.

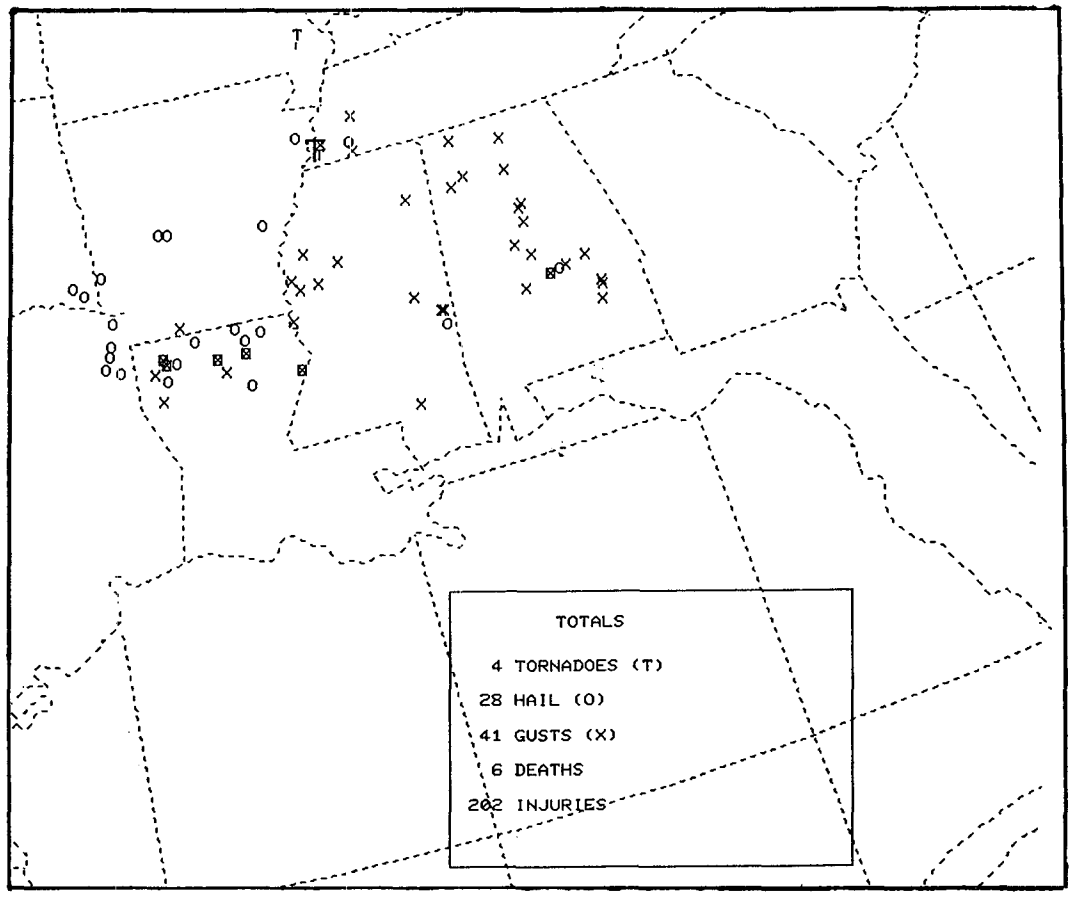

FIG. 3. As in Fig. 2, except from 1200 UTC 14 December 1987 to 1200 UTC 15 December 1987.

Therefore, only anticyclones with displacement errors of 100 km or greater are included in the directional error statistics. Eleven percent of the predicted NGM anticyclones were within 100 km of the observed location, compared with 6% of the AVN forecasts and 3% of the LFM forecasts.

The directional errors for the 48-h predictions for each model are shown in Fig. 5. Little directional bias is noted in the errors of the NGM and AVN models, although the NGM displayed a slight tendency to predict anticyclone centers west of the observed position. The LFM, however, showed a marked tendency to move anticyclones eastward too rapidly, with 41% of the forecasts east of the verifying position. Nearly nine-tenths of the LFM forecasts were south or east of the observed location.

The LFM and AVN directional errors are similar to the findings of Grumm and Gyakum (1986, hereafter GG) for their Atlantic southeast (AS) region (which corresponds most closely to the geographic domain of this study), except the current data show a somewhat greater tendency for the LFM to forecast anticyclones too far south and east. The NGM directional errors are also similar to those recently reported by Grumm and Siebers (1989b, hereafter GS), who examined surface anticyclone errors in the NGM during the period December 1988–August 1989. Although their data sample and geographic domain were substantially larger, they also noted considerable scatter of the NGM directional errors in the winter.

Mean displacement errors and frequency distributions are shown in Fig. 6. The NGM had the smallest mean error of 287 km, while the AVN error was only slightly larger at 302 km. The LFM had the largest mean error of 411 km. The errors for the AVN and LFM are smaller than the displacement errors of GG in their AS region; both results, however, indicate the higher skill level of the AVN compared to the LFM. Substantial improvement in the model formulation of the AVN since 1982 may account for much of the increase in AVN accuracy. Nevertheless, the LFM has been a relatively stable model during the 1980s, which suggests that differences in data sample and geographic domain may also contribute to the smaller displacement errors in this study.

The mean NGM displacement error of 287 km is much smaller than the mean winter error of 448 km reported by GS. However, their winter sample showed

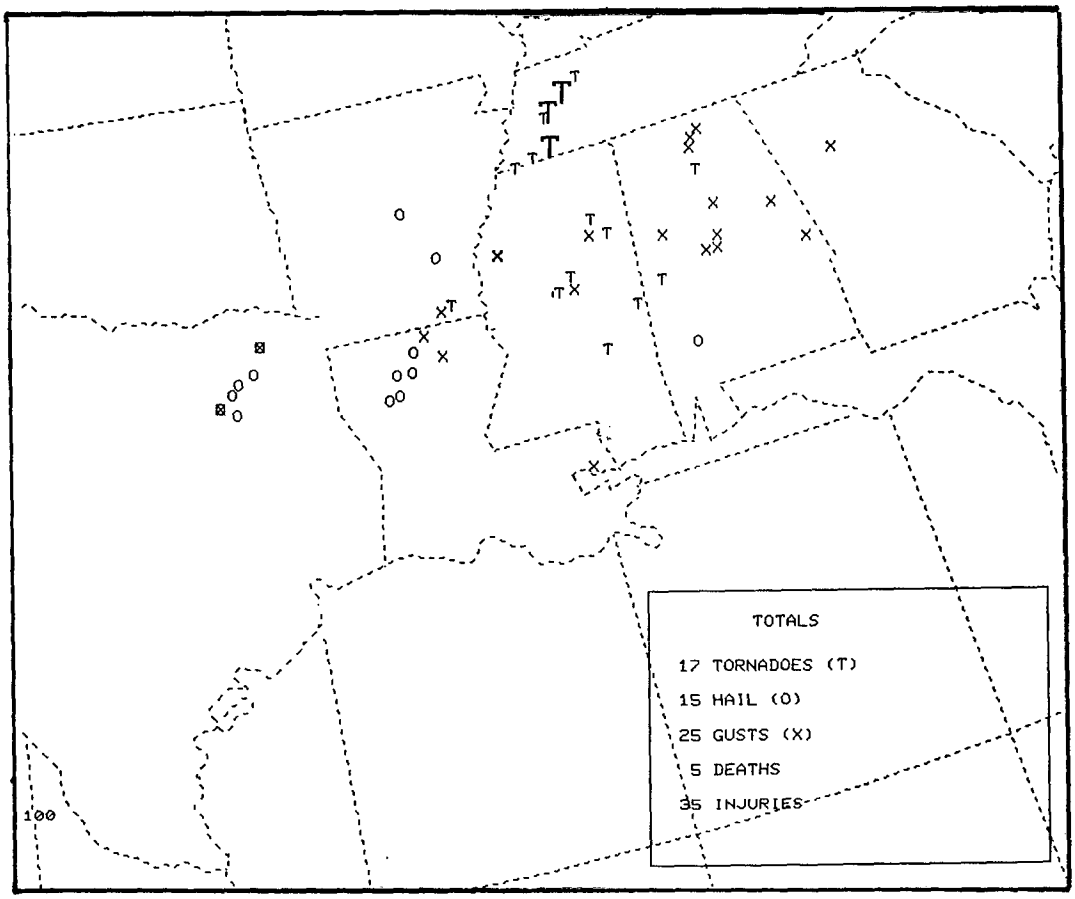

FIG. 4. As in Fig. 2, except from 1200 UTC 18 January 1988 to 1200 UTC 20 January 1988.

a preponderance of anticyclones over the elevated terrain of western North America. Since that geographic region was not included in the GUFMEX study, the displacement results are not directly comparable.

While mean statistics provide useful information, frequency distributions of the displacement errors provide additional insight into model performance (Fig. 6). The NGM and AVN have similar error distributions with relatively few errors larger than 500 km. The LFM displays a broader distribution indicative of less reliability compared to the other models.

To examine the possible relationship between anticyclone displacement and directional errors, the errors were combined on scatter diagrams for each model. These diagrams (not shown) did not reveal any apparent correlation between the two types of errors. In general, distance errors tended to be randomly scattered along each radial sector without evidence of clustering. Thus, the limited sample of anticyclone cases does not suggest that large distance errors for any model are associated with a particular direction. Since the directional errors for the AVN and NGM were well distributed in all directions, the very small data sample available for each sector precludes a thorough statistical analysis of the combined displacement and direction errors.

TABLE 1. Numerical model data sample.

Outbreak case	Model evaluation period		Number of model runs
	Start	End	
15–16 November 1987	0000 UTC 9 November	1200 UTC 15 November	14
14 December 1987	1200 UTC 5 December	1200 UTC 15 December	21
18–19 January 1988	1200 UTC 9 January	1200 UTC 17 January	17

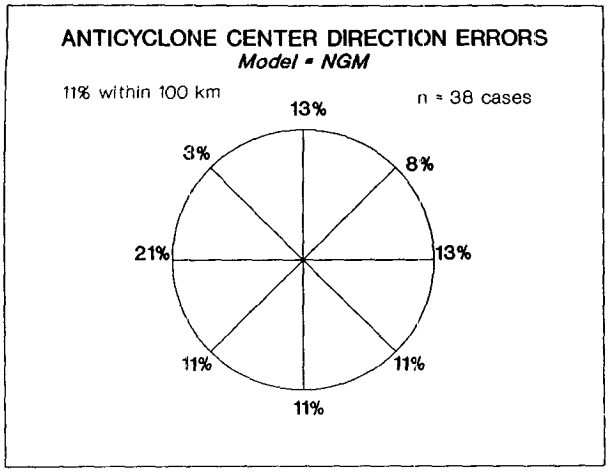

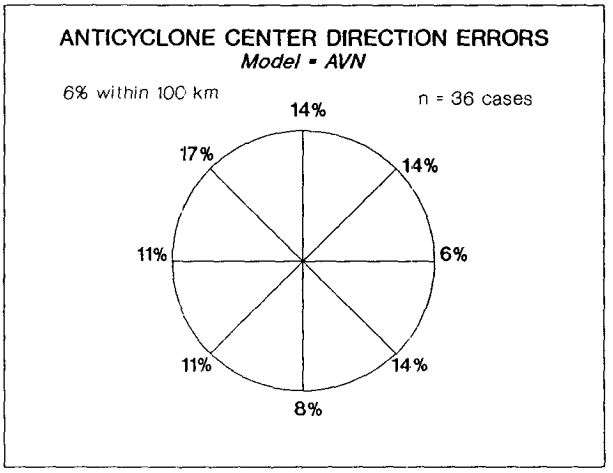

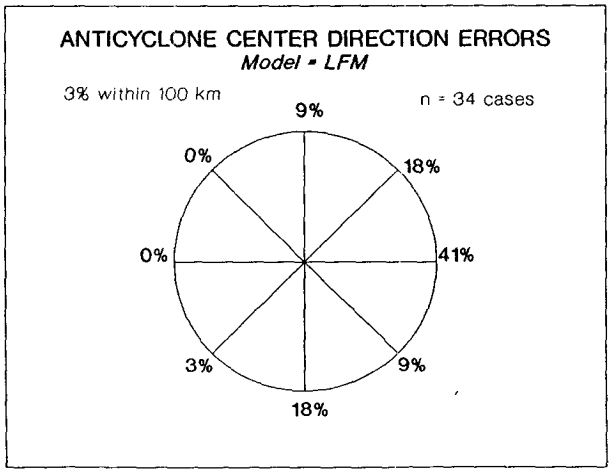

FIG. 5. Distribution of anticyclone directional errors for 48-h forecasts from NGM (top), AVN (middle), and LFM (bottom). North is at the top of each circle. Error is defined as direction of forecast anticyclone with respect to observed anticyclone.

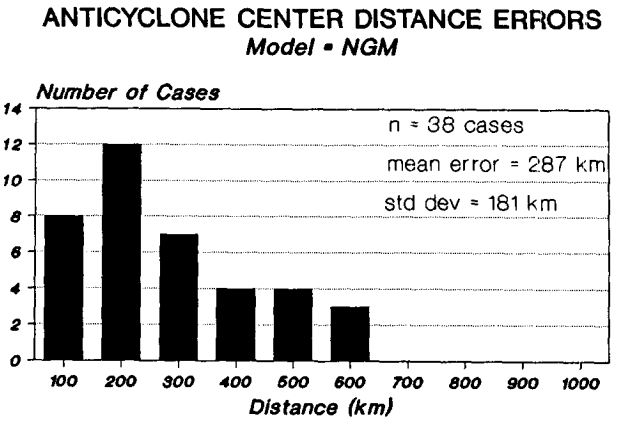

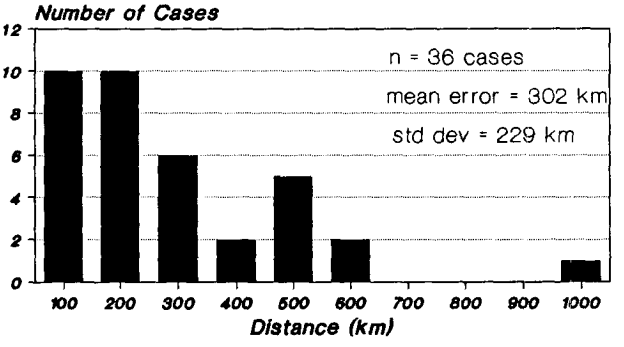

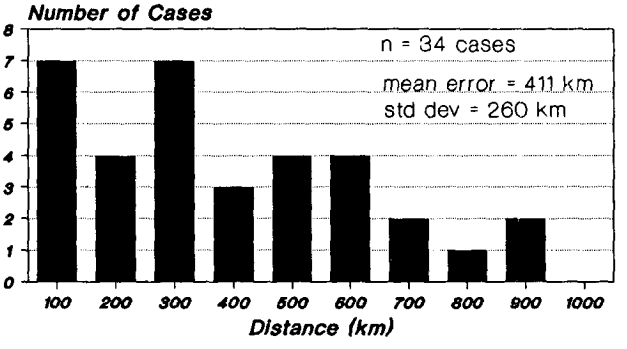

FIG. 6. Distribution of anticyclone displacement errors (km) for 48-h forecasts from NGM (top), AVN (middle), and LFM (bottom).

Mean anticyclone central-pressure errors and frequency distributions are displayed in Fig. 7. All models showed a tendency to underforecast the anticyclone pressure, with the AVN and NGM having small mean

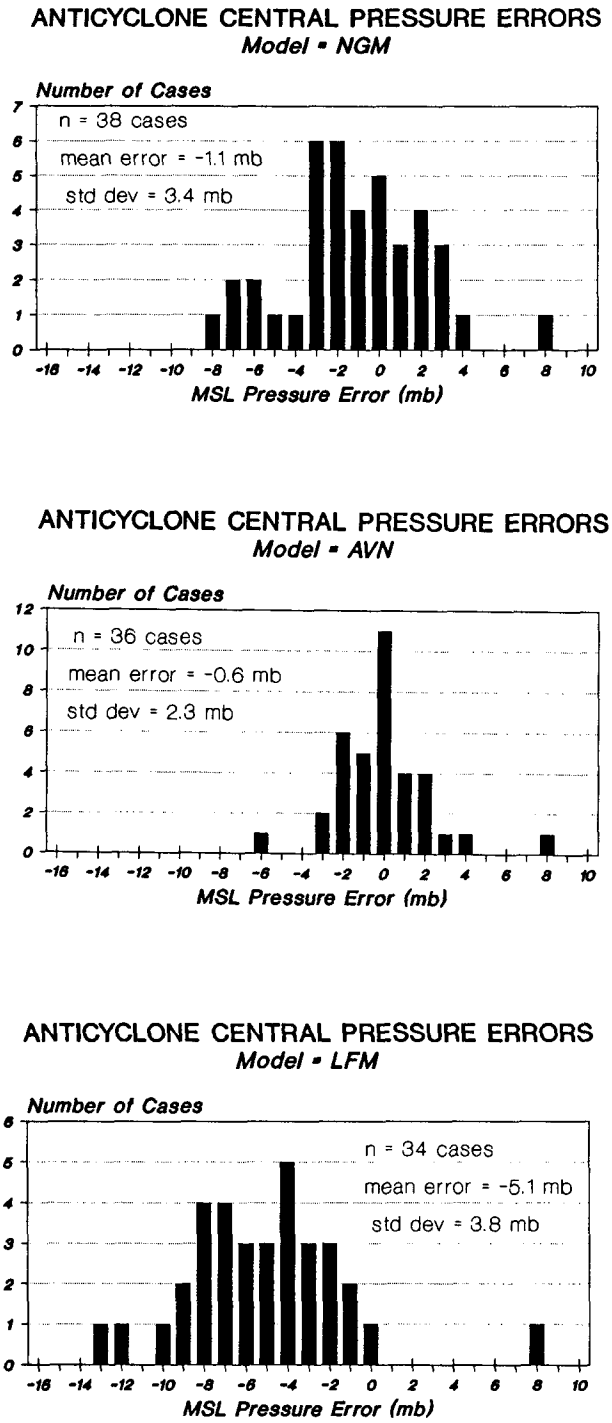

FIG. 7. Distribution of anticyclone central-pressure errors (mb) for 48-h forecasts from NGM (top), AVN (middle), and LFM (bottom). Error is defined as forecast pressure minus observed pressure.

errors of −0.6 and −1.1 mb, respectively. This is similar to the error distribution of GS that indicated the NGM tends to underforecast the central pressure over much of the central and eastern United States in the winter. The LFM tended to underforecast the pressure substantially, averaging 5-mb errors at the 48-h projection. The frequency distributions (Fig. 7) confirm the higher skill level of the AVN, which displays a relatively narrow error distribution centered near zero. The NGM has a broader error distribution than the AVN, while the LFM errors are displaced markedly to the left (negative) side of the histogram. These results are comparable to the LFM and AVN anticyclone pressure errors found by GG in their AS region, except the mean underforecast error of the LFM in this study is about twice the error reported by GG.

Finally, it is not uncommon during the cool season for well-defined surface ridge axes to extend from the eastern United States southwestward toward the northern Gulf. In these cases the location of the ridge axis is an important factor that influences the onset of return flow over the northwest Gulf, even when a primary anticyclone center is not predicted by the model. Accordingly, the model forecasts were examined to identify cases when observed anticyclone centers were not explicitly predicted (e.g., no labeled center), but a well-defined ridge axis was forecast. Table 2 shows that when observed anticyclone centers were not predicted, the NGM and AVN had forecast a ridge axis within 200 km of the observed axis in nearly nine-tenths of the cases. The LFM displayed less skill in these situations, properly locating the ridge axis in only about one-third of the cases.

b. Prediction of surface pressure along the Gulf coast

Since the focus of the GUFMEX return-flow investigations was the northwest Gulf region, it was also important to determine model forecast skill in predicting surface (MSL) pressure along the Gulf coast. Studies of operational model performance have noted a tendency for baroclinic models to lower surface pressures excessively east of the Rocky Mountains (e.g., Fawcett 1969; Schecter 1984). This underforecasting bias was found to be especially noticeable during cyclogenesis in the lee of the mountains (Leary 1971; Silberberg and Bosart 1982; Grumm and Siebers 1989a; Mullen and Smith 1990).

In this study 48-h surface-pressure forecasts were evaluated along the Gulf coast at Brownsville, Texas (BRO), Galveston, Texas (GLS), and just south of New Orleans, Louisiana (NEW). The predicted pressure from each model at these locations was compared

TABLE 2. 48-h model predictions of ridge-axis location when anticyclones are not forecast explicitly.

	Observed but not forecast	Ridge axis within 200 km of verifying center
NGM	7	6
LFM	11	4
AVN	8	7

TABLE 3. Gulf coast pressure errors (mb, MSL) for 48-h model forecasts.

	BRO	GLS	NEW	All cases	Number
NGM	−0.8	−1.5	−1.2	−1.1	156
LFM	−7.5	−8.6	−7.0	−7.7	156
AVN	−0.4	−0.5	−0.3	−0.4	150

with the observed pressure on the 00-h NGM verifying analysis for all data periods in the sample. As seen in Table 3, all models showed a tendency to underforecast the pressure along the coast. It is interesting that the Gulf coast mean pressure errors were very similar to the model anticyclone mean central-pressure errors (Fig. 7), with the AVN again having the smallest error and the LFM the largest. Note that the NGM and AVN mean errors along the Gulf coast are nearly identical to the respective model pressure errors at the center of the anticyclone. In contrast, the LFM errors represent underforecasts that are more than 2 mb larger along the coast than at the anticyclone center, averaging nearly 8 mb too low at the 48-h projection. This implies that a stronger southerly pressure gradient tends to accompany the low surface-pressure bias in the LFM.

The individual station statistics show the largest pressure errors occurred at GLS for all three models. The fact that the largest errors were along the northwest Gulf coast may be related to the closer proximity of GLS to the plains, where model underforecast errors are typically maximized.

Frequency distributions of the 48-h coastal pressure errors (Fig. 8) depict the relative superiority of the AVN forecasts as well as the systematic underforecasting of pressure in the LFM. The AVN error distribution is more clustered near zero than are the NGM errors, while the LFM errors are noticeably shifted to the negative side of the histogram. These results are very similar to the central-pressure error distribution shown in Fig. 7.

The pressure errors found in the LFM are consistent with other studies that documented large model underforecast errors east of the Rockies (e.g., Schecter 1984). It is also important to recognize that the LFM errors occur not only when cyclones develop in the plains, but also with anticyclones. For example, when the LFM overdeepens a cyclone in the lee of the Rockies (Fig. 9) the erroneous lowering of surface pressures in the Great Plains extends into the northwest Gulf. Although the AVN and NGM also underpredicted pressures in the northern and central plains (but not as much as the LFM), their underforecast errors were substantially reduced along the Gulf coast, where both the AVN and NGM properly maintained a strong ridge axis that prevented the "opening" of the Gulf to moisture return.

In a different pattern shown in Fig. 10, all three models correctly predicted an anticyclone building southeastward across the Great Plains into the Gulf. In this example the LFM weakened the anticyclone too rapidly and also underforecast pressures along the Gulf coast by about 8 mb. Reasonably correct pressure

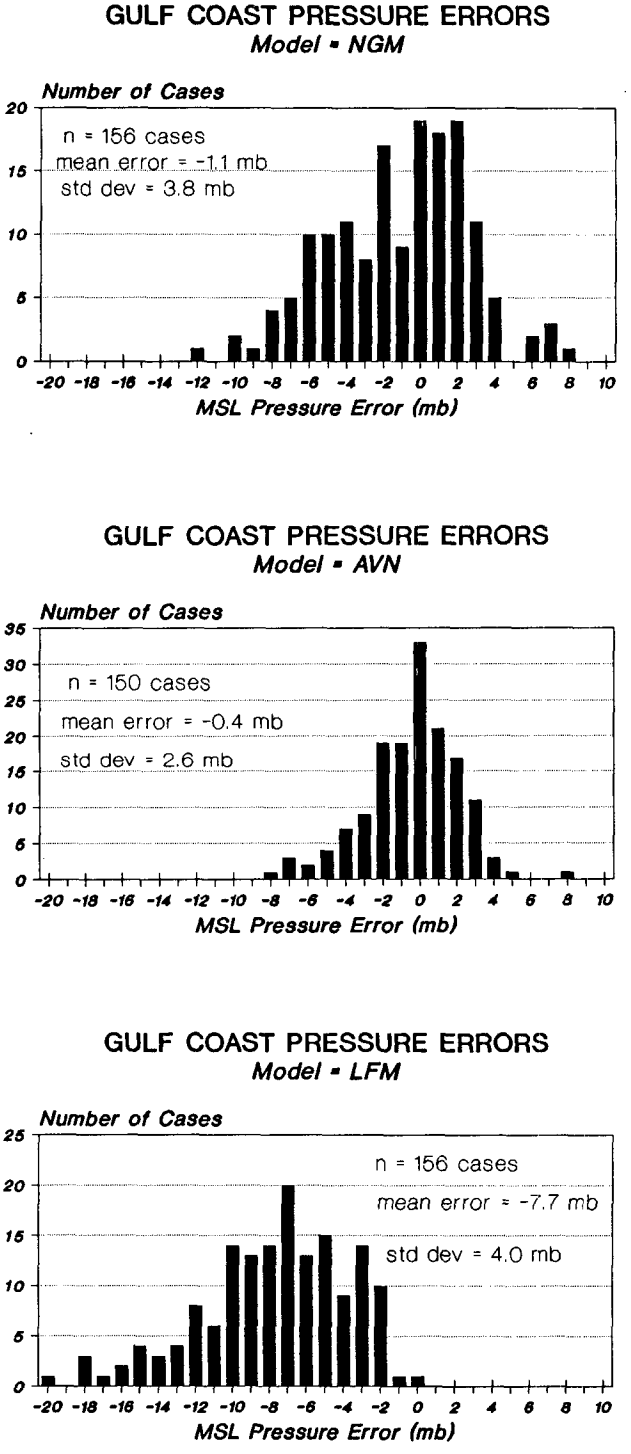

FIG. 8. Distribution of Gulf coast pressure errors (mb) for 48-h forecasts from NGM (top), AVN (middle), and LFM (bottom). Error is defined as forecast pressure minus observed pressure.

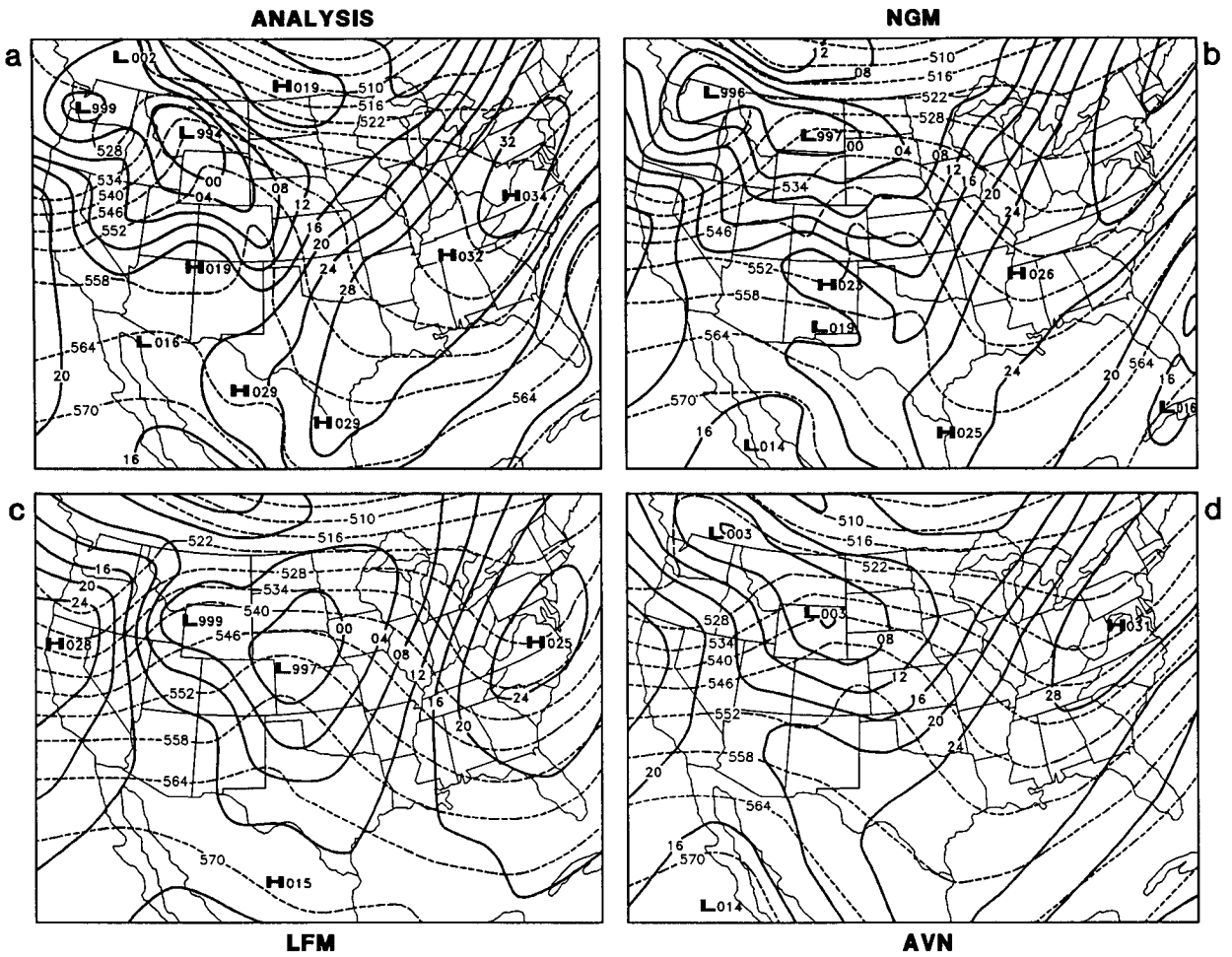

FIG. 9. MSL pressure (mb, solid) and 1000–500-mb thickness (dam, dashed) for 1200 UTC 11 January 1988 from (a) 00-h NGM, (b) 48-h NGM, (c) 48-h LFM, and (d) 48-h AVN.

forecasts along the coast were produced by the AVN and NGM.

c. *Prediction of cold fronts moving into the Gulf*

Six cold fronts moved across the southern plains into the Gulf of Mexico during the period of study. Three of the fronts moved across the Loop Current over the southeast Gulf and into the Caribbean Sea, two fronts entered the northern Gulf and became diffuse, and one front entered the northwest Gulf where it became diffuse. Although this sample is admittedly quite small, it appears representative of the typical Gulf cold-front climatology described by Henry (1979), who found that the majority of cold-season fronts moved into the Caribbean before they underwent frontolysis.

In general, after entering the Gulf most cold fronts were not associated with an explicit pressure trough on the model charts. As seen in Fig. 10, this was true for the 48-h forecasts from all three models and the 00-h NGM verifying analyses. Therefore, the combination of pressure patterns and 1000–500-mb thickness displayed on the forecast charts was used to locate frontal positions in the Gulf subjectively. When present, the leading edge of a well-defined thickness gradient can approximate the location of the surface front (Saucier 1955). During GUFMEX an accurate prediction of the *exact* location of a cold front was not typically needed, since the airmass modification investigation required only that polar air be over the Loop Current. Thus, it was not necessary to know how far south and east of the Loop Current the cold front would be, but only that the front had moved across the warm gyre.

Overall, there appeared to be little difference in the quality of the model predictions, with the LFM, AVN, and NGM all displaying moderate skill in forecasting the movement of cold fronts across the Gulf.

d. *Prediction of return flow over the western Gulf*

An analysis of the development of onshore flow and the subsequent return of Gulf moisture toward the coast

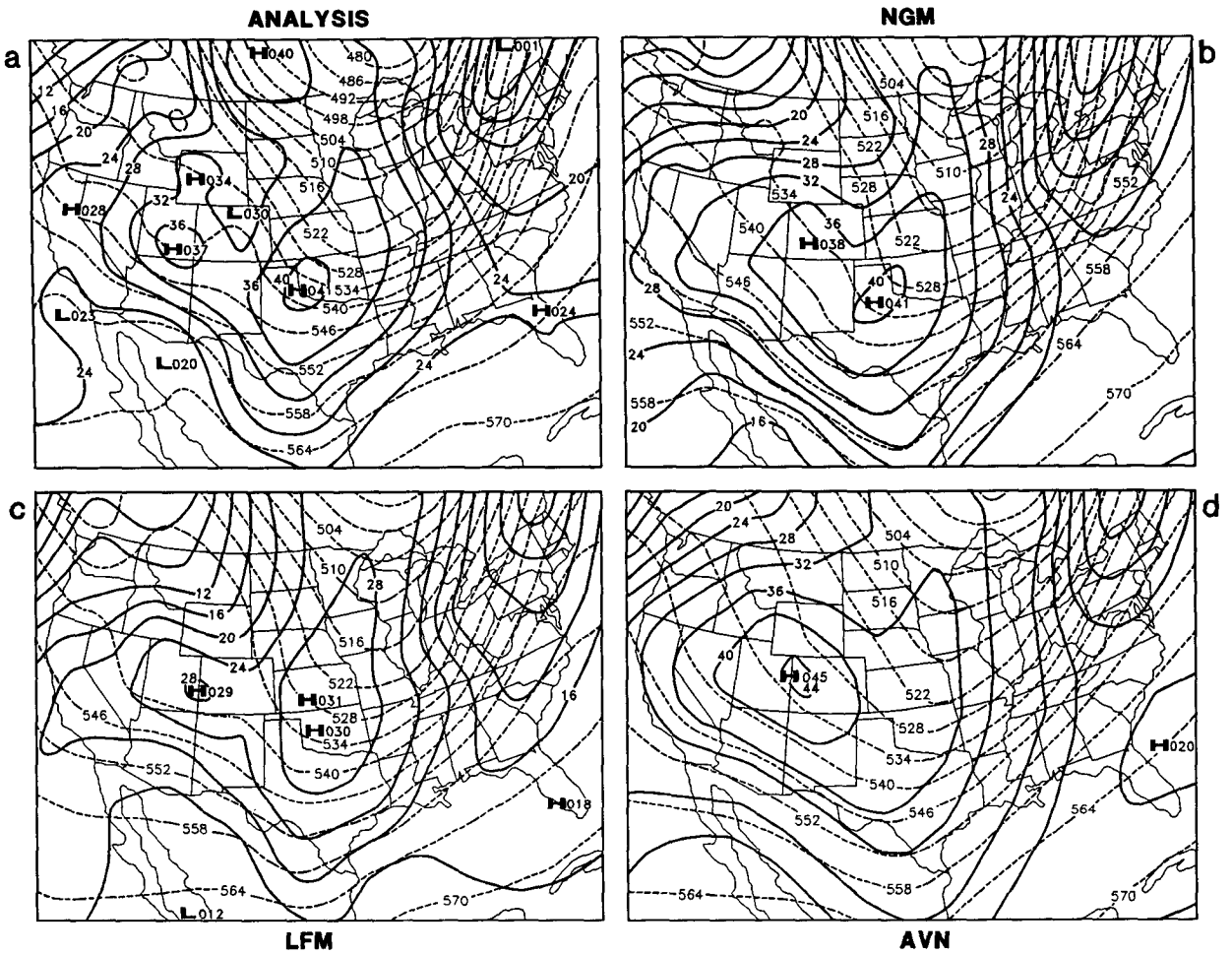

FIG. 10. As in Fig. 9, except for 1200 UTC 13 January 1988.

is a key facet of GUFMEX. For the purposes of this study, return flow is considered to exist when a surface isobar (4-mb interval) crosses the coastline between Brownsville and Apalachicola, Florida, producing a southerly component to the geostrophic wind. This definition is useful in the context of synoptic pattern correlation, since the determination of actual moisture return to the continent was beyond the scope of this study. This definition also satisfied a primary goal of forecasters during the cold season, which is the identification of synoptic patterns that tend to be associated with moisture return from the Gulf.

Application of this definition to the NGM 00-h verifying analyses and the 48-h predictions from the three models allowed a comparison of the observed frequency of occurrence of return flow over the Gulf coast with the predicted frequency of occurrence by each model. Return flow was present on 28 of the verifying analyses, and the NGM and AVN tended to predict the frequency of occurrence correctly, with 27 and 26 forecasts, respectively. The LFM, however, substantially overpredicted the occurrence with 40 forecast charts depicting return flow. This is consistent with earlier results showing the LFM tends to lower pressures excessively east of the Rockies and extending southward to the Gulf coast.

The forecasting of the onset of return flow was also examined, since this is a key consideration for operational forecasters. Four return-flow episodes developed for the three cases. Return flow developed twice for the January 1988 case. The first onset lasted for only a brief time before a second cold front moved into the Gulf. The severe outbreak in this case was associated with the second return-flow episode.

The onset of return flow for the verifying or forecast times was defined as the first occurrence that satisfied the return-flow definition. As seen in Table 4, the AVN correctly predicted the onset of all four episodes, while the NGM was correct on three episodes and 12 h (one model run) too late on the other episode. The LFM predictions were quite premature in all cases, with the errors ranging between 24 and 36 h too early. An example of the LFM opening the Gulf prematurely is shown in Fig. 9.

Finally, the spatial extent of the return-flow circulation was examined. The eastern limit of return flow is defined as the easternmost model isobar (4-mb interval) that met the return-flow criterion. When the western Gulf was observed to be open (return flow in progress) the areal extent of the predicted return flow was compared with the verifying analyses. Results in Table 5 indicate a tendency for the NGM and AVN to forecast the eastern extent slightly too far west, while the LFM shows a pronounced tendency to open the Gulf too far east. This is consistent with earlier findings that the NGM and AVN sometimes place surface anticyclones west of the observed position with occasional positive pressure errors along the Gulf coast. The LFM results are also consistent with its biases of moving anticyclones too rapidly eastward and lowering pressures excessively along the coast. An example of the LFM overdeveloping return flow is shown in Fig. 11.

5. Severe-weather outlooks during GUFMEX

Even when the overall synoptic pattern indicates the likely development of return flow over the western Gulf, the prediction process is hampered by a lack of data over the Gulf. Thus, reliable quantitative information about the moisture content and stability of the return-flow air mass is not available until after the airmass has reached the coast and can be sampled by coastal rawinsondes. It is interesting that this aspect of the forecast problem was recognized by forecasters in the early days of severe local storm forecasting (U. S. Weather Bureau 1956).

To investigate the impact of low-level moisture and airmass stability on operational severe-thunderstorm forecasting, the severe local storm (or convective) outlooks issued during GUFMEX by the severe local storms (SELS) unit at NSSFC were examined. SELS issues second-day (day 2) outlooks at 0800 and 1800 UTC for the 24-h period beginning at 1200 UTC the next day. A first-day (day 1) outlook is issued at 0700 UTC for the 24-h period beginning at 1200 UTC, and is updated at 1500 and 1900 UTC. These outlooks delineate areas of severe-thunderstorm potential over the contiguous United States.

During the 51-day period of this study SELS outlooks included a risk of severe thunderstorms on less than half of the days, ranging from 16 severe outlooks on the initial day 2 issuance to 22 severe outlooks on the afternoon day 1 forecast (Table 6). One or more severe events were reported on about half (26) of the days. However, SELS outlooks are not intended to forecast the occurrence of an isolated severe event. Thus, it may be more meaningful to also identify days when at least two severe events occurred, which included 41% of the days. Note that this relative frequency of occurrence is quite similar to the relative frequency of severe outlook issuance, suggesting that most outlooks displayed no apparent over- or underforecasting bias. If a bias does exist, it occurred on the initial day 2 outlook, which tended to slightly underforecast the frequency of severe-weather days. This most likely reflects the greater uncertainty that accompanies forecasts with longer lead times.[1]

As seen in Fig. 12, verification statistics of critical success index (CSI), probability of detection (POD), and false-alarm ratio (FAR) indicate the outlooks generally became more accurate on each update, with most of the improvement evident between the first day 2 outlook and the first day 1 outlook. These results are similar to the long-term statistics presented by Leftwich (1989) for all of 1988, which indicated that the SELS outlook performance tends to improve as the lead time of the forecast decreases.

TABLE 4. Temporal errors (h) in the onset of return flow. Error = forecast − observed. Negative (positive) errors mean the onset was predicted too early (late).

	−36	−24	−12	0	+12
NGM	0	0	0	3	1
LFM	2	2	0	0	0
AVN	0	0	0	4	0

TABLE 5. Spatial errors in the eastern extent of return-flow forecasts. Error = forecast − observed. Negative (positive) errors mean the return flow was predicted too far east (west).

	Number of forecasts	Mean error (deg long)
NGM	19	+0.9
LFM	25	−4.2
AVN	19	+1.8

6. The relationship between thermodynamic fields and outlook performance

The SELS outlooks also suggest that limitations on the predictability of late winter–early spring severe local storm episodes may be influenced strongly by the airmass changes associated with return-flow situations.

[1] This is because SELS forecasters generally have a conservative philosophy when assessing the severe-thunderstorm risk on the day 2 outlooks. It has been observed that forecasters are typically reluctant to remove a low-confidence risk area issued on the initial day 2 outlook, even if they believe it is not the best forecast. This aspect of hedging (Murphy and Winkler 1971) can be related to a number of factors, including the inability of the forecaster to definitively rule out the threat of severe thunderstorms, the desire to maintain a degree of consistency in a series of forecasts valid for the same time period, and the categorical (rather than probabilistic) formulation of the outlook (Murphy 1991). As a result, it is "easier" for the forecaster to add a new severe-risk area on later outlooks than it is to remove an existing risk area. In light of this reasoning, a conservative approach has evolved in the issuance of day 2 outlooks, with the greater uncertainty resulting in the issuance of fewer severe-risk areas.

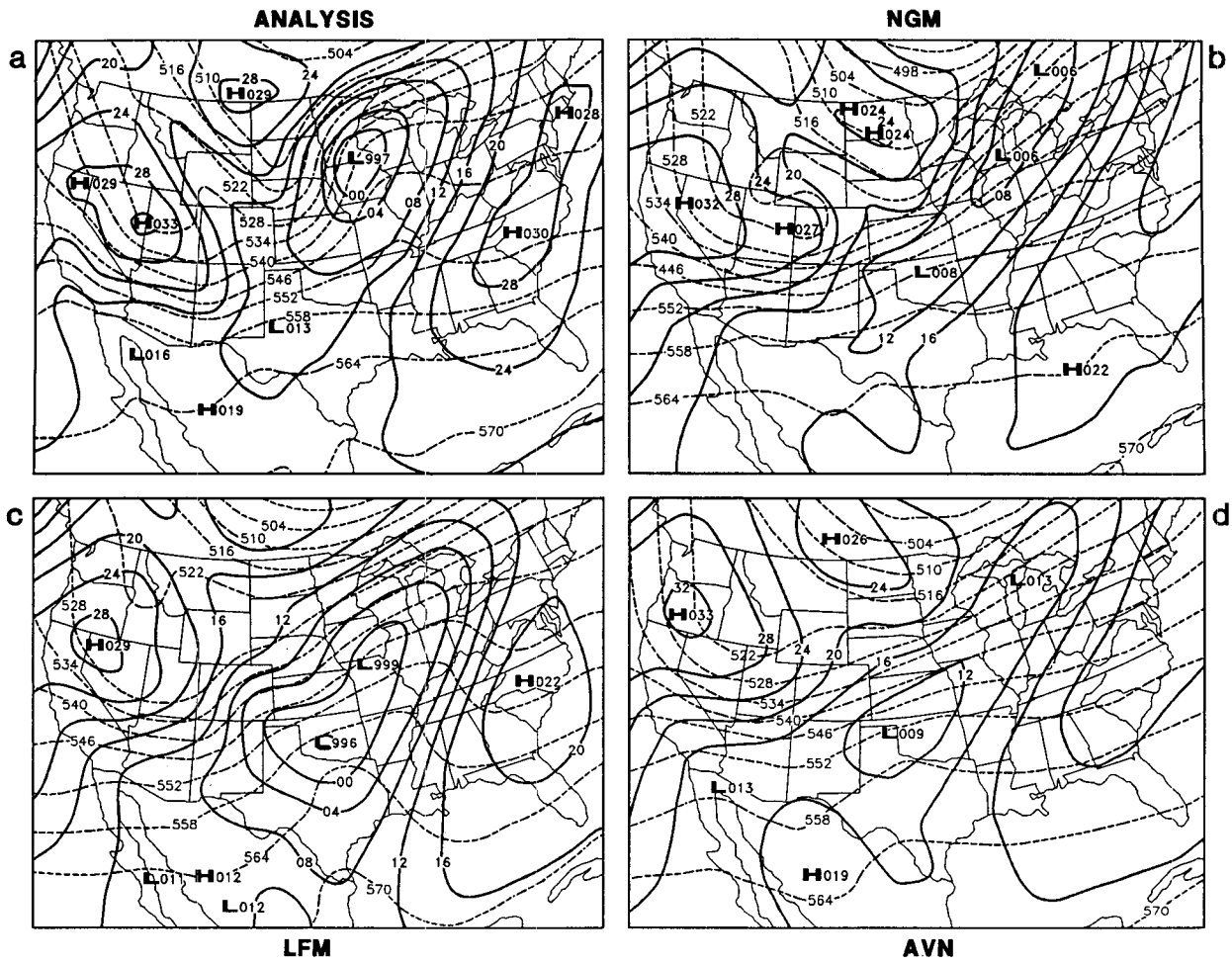

FIG. 11. As in Fig. 9, except for 1200 UTC 12 January 1988.

For example, inspection of the narrative discussions included in the initial day 2 and initial day 1 outlooks reveals that the return of moisture is a primary forecast problem during this time of year. In nearly 40% of the day 2 discussions and more than 60% of the day 1 discussions the return of low-level moisture was mentioned explicitly as a key forecast decision. An example can be found in the day 2 outlook discussion issued 29 February 1988:

Short wave troughs in both northern and southern branches of westerlies come into phase over Rockies during the period. Since southern short wave likely to be rather weak, expect most of the surface development to be from the northern plains northward. *Slowly increasing southerly flow over the southern high plains likely to begin advecting low-level moisture northward during the day with instability increasing to marginally unstable values by 00Z March 2.* Rather strong westerly mid-level winds forecast across west Texas by 00Z will result in favorable directional shear from the surface to 500 mb. Upward vertical motion is indicated ahead of the cold front as it moves into the southern plains during the late afternoon and evening hours. Therefore, expect thunderstorm activity to develop by late afternoon near the New Mexico/Texas border and move eastward into west Texas during the evening hours. A few cells may approach severe limits. However, mar-

TABLE 6. Relative frequency of occurrence and prediction of severe weather during GUFMEX. Numbers in parentheses refer to percentage of total days.

Total days	Days with ≥ 1 severe events	Days with ≥ 2 severe events
51	26 (51)	20 (41)

Number of severe outlooks (All times UTC)

DAY2		DAY1		
0800	1800	0700	1500	1900
16 (31)	20 (41)	19 (37)	20 (41)	22 (43)

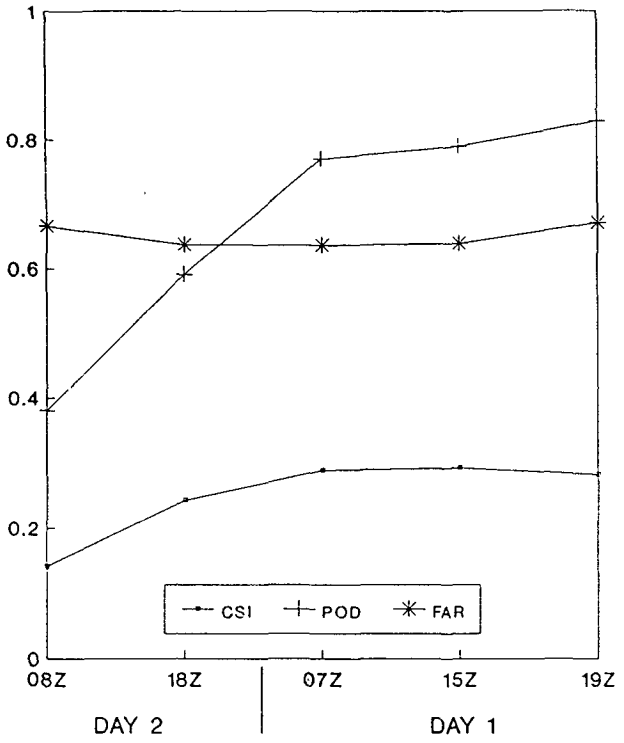

FIG. 12. Verification statistics of critical success index (CSI), probability of detection (POD), and false-alarm ratio (FAR) for SELS outlooks during the GUFMEX period (15 February–4 April 1988).

ginal instability is likely to preclude severe development. *Will need to monitor the low-level moisture return closely.*

Since large-scale forcing for vertical motion associated with baroclinic waves occurs frequently during the late winter and early spring, the limiting factor for severe local storms is often the availability of moisture and potential instability. Unfortunately, the data void over the Gulf impacts both the human forecaster and the operational numerical weather prediction models in predicting changes in moisture and stability. This impact may be greatest for the longer-range forecasts such as the day 2 outlook. These products rely more heavily on guidance from the numerical models than do the day 1 outlooks, which reflect a combination of diagnostic analysis techniques supplemented by prognostic output from numerical models. It is hypothesized that when return-flow moisture is located over the Gulf, model forecasts of stability and the resultant operational severe-storm forecasts tend to be less skillful compared to situations when the moisture has spread inland already. To test this hypothesis, the performance of the initial day 2 outlooks during GUFMEX was compared with 1) antecedent conditions of low-level moisture and airmass stability at coastal rawinsonde sites in Texas and Louisiana, and 2) 48-h lifted-index predictions from the NGM.

a. Diagnostic evaluation of moisture and stability

Statistical verification scores were used to stratify the day 2 outlook performance into "good" and "bad" categories. In particular, the CSI was used as the measure of skill. Good outlooks are defined as having a CSI of 0.30 or greater and consisted of outlooks that accurately delineated the location of severe-storm events.[2]

Bad outlooks are defined as having a CSI of less than 0.22. To better understand the forecast errors that contribute to outlooks with low CSI scores, the bad outlooks can be subdivided into three categories.

1) The outlook delineated a severe-thunderstorm risk area but no severe events were reported. These are called "false-alarm" outlooks.

2) The outlook predicted no severe thunderstorms would occur, but severe events were reported in an organized spatial pattern. These are called "failure-to-predict" outlooks.

3) The outlook delineated a severe-thunderstorm risk area and severe events occurred in an organized spatial pattern. However, the risk area was incorrectly located (low POD) and/or covered much too large an area (high FAR).

Note that the first category consists of bad outlooks when no severe thunderstorms developed, while the latter two categories describe bad outlooks when organized areas of severe thunderstorms occurred.

The stratification of the initial day 2 outlooks by CSI performance resulted in 6 good outlooks and 12 bad outlooks. (One outlook was judged intermediate in skill.) The contrast in outlook performance was most noticeable between the 6 good outlooks that accurately delineated the occurrence of severe events (and had a mean CSI of 0.544) and the 5 bad outlooks that predicted severe thunderstorms when none occurred (the false-alarm outlooks, which all had a CSI of 0.000). The low-level moisture and airmass stability present along the Texas and Louisiana coasts at 0000 UTC prior to the issuance of the outlooks were examined, since these parameters can be used to identify some of the characteristics of the return-flow air mass. The pa-

[2] It should be mentioned that a correct forecast of no severe events should also be considered a good outlook. These are difficult to evaluate in a statistical sense because the CSI algorithm (Donaldson et al. 1975) does not incorporate this forecast–occurrence combination. This is not a problem on some occasions, since many of the none-forecast–none-occurred outlooks are trivial during the cool season when a stable air mass covers the nation. However, some of these cases do require considerable skill to forecast correctly, but the CSI gives no credit in these instances. Another measure of skill for rare-event forecasting, the Heidke skill score, does incorporate the none-forecast–none-occurred category in a controlled fashion and is discussed in detail by Doswell et al. (1990a,b).

rameters from rawinsondes at Brownsville, Texas, Victoria, Texas, Lake Charles, Louisiana, and Boothville, Louisiana, included the mean mixing ratio q in the lowest 100 mb, the 850-mb dewpoint temperature T_d, the SELS lifted index (LI—Galway 1956), and the Showalter stability index (SSI—Showalter 1953).

As seen in Table 7, it appears that substantially different air masses were present along the coast prior to the issuance of good outlooks versus the false alarm outlooks. According to the LI and q data an unstable air mass with ample low-level moisture was in place along the coast prior to the issuance of good day 2 outlooks. Conversely, these data indicate that a relatively dry, stable air mass was present prior to the issuance of the false-alarm outlooks. Table 7 also suggests that the LI and q parameters reflect the subsequent thunderstorm potential better than the 850-mb T_d and the SSI. Note that prior to the issuance of the good outlooks, the mean LI was negative and q was relatively high, which is consistent with increasing thunderstorm potential. On the other hand, the positive SSI and low 850-mb T_d preceding the good outlooks do not appear favorable for significant convection. When the false-alarm outlooks are considered, none of the mean parameters appears supportive of strong convective potential.

The LI and q parameters demonstrate some ability to differentiate between the air mass along the coast prior to the issuance of good outlooks and the coastal air mass prior to false-alarm outlooks, and they accomplish this distinction with physically realistic parameter values. Although the SSI and 850-mb T_d also appear to differentiate between the two outlook categories, dry and stable air masses are associated with both categories. This is not unexpected, since low-level moisture is occasionally below 850 mb during some cool-season return-flow episodes. These data suggest that the potential for severe-thunderstorm development is influenced by the antecedent thermodynamic environment present along the Gulf coast at least 36 h prior to the start of the forecast period.

b. Prediction of airmass stability by the NGM

The formulation of the day 2 outlook is influenced strongly by model guidance, since output from numerical models typically provides significant input to forecasts beyond the 12–24-h time frame. Predictions of airmass stability, which is a key thermodynamic parameter used in severe-thunderstorm forecasting, were obtained from the NGM four-layer lifted-index forecasts. The NGM 48-h lifted-index forecasts for 0000 UTC are valid at the midpoint of the day 2 outlook period and are representative of the time interval when severe thunderstorms and tornadoes are favored climatologically (Kelly et al. 1978; Kelly et al. 1985). The 48-h lifted-index predictions were compared with the verifying 00-h initial-analysis lifted-index fields for the good outlooks and the false-alarm outlooks to determine if any differences in model performance could be identified. The contoured lifted-index fields were manually transformed to a 2° latitude × 2° longitude grid covering much of the south-central and southeastern United States east of the Rockies, and 48-h forecast errors were computed.

Model forecasts that provided input to the five false-alarm outlooks were associated with lifted-index errors that were more than 2°C too unstable when averaged over the grid (Fig. 13). The largest mean errors were over the lower Mississippi Valley and Tennessee Valley where the NGM lifted-index forecast was excessively unstable by 8°C. As indicated in Fig. 13, the false-alarm outlook areas also were centered over the region with the largest lifted-index errors, suggesting that forecasters were influenced strongly by the erroneous lifted-index predictions. An example of one GUFMEX case when the NGM substantially overforecast the degree of instability is shown in Fig. 14. The cases in this small sample during GUFMEX displayed lifted-index

TABLE 7. Mean conditions at 0000 UTC prior to issuance of day 2 outlooks.

	Brownsville				Victoria				Lake Charles				Boothville				All				Total
	LI	Q	SSI	$T_{d\,850}$	LI	Q	SSI	$T_{d\,850}$	LI	Q	SSI	$T_{d\,850}$	LI	Q	SSI	$T_{d\,850}$	LI	Q	SSI	$T_{d\,850}$	cases
Good outlooks	−3.5	14.0	2.0	6.0	−2.3	10.1	−2.2	6.8	−0.8	9.7	5.7	1.2	0.2	9.3	5.4	1.3	−1.6	10.6	2.8	3.1	6
False-alarm outlooks	1.8	9.4	6.0	0.2	2.8	7.0	5.8	−0.6	5.6	7.0	8.0	−3.8	5.8	7.1	9.4	−5.0	3.2	6.0	7.3	−2.3	5
Bad outlooks when severe occurred	−0.7	11.1	3.3	4.0	−1.3	9.3	3.9	0.4	−2.7	11.1	5.0	0.8	0.7	9.6	2.7	5.0	−1.0	10.3	3.7	2.6	7

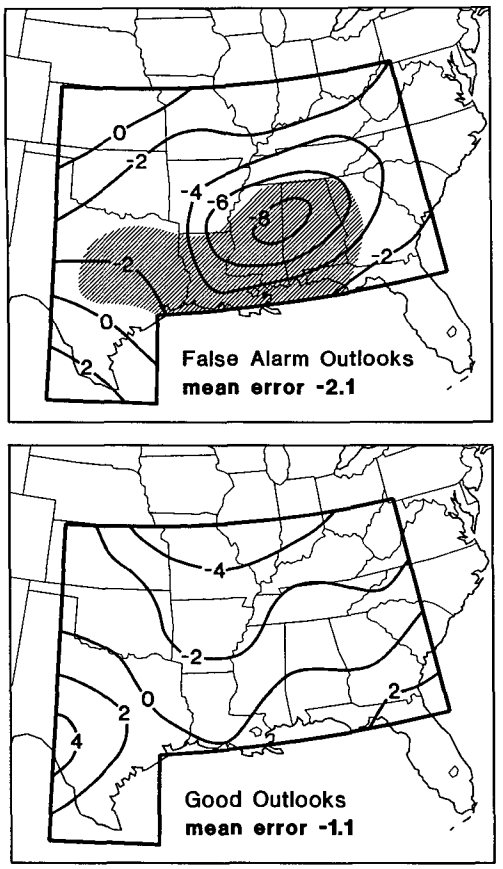

FIG. 13. NGM 48-h lifted-index mean errors (°C) for false-alarm day 2 outlooks (top), and for good day 2 outlooks (bottom). Error is defined as forecast minus observed. Hatching denotes composite region of severe-risk forecast areas for false-alarm outlooks.

errors similar to those reported by Weiss (1987), who found that the NGM exhibits little skill in predicting areas of extreme instability.

An analysis of the lifted-index prediction errors for the six good outlook cases is also shown in Fig. 13. The average error over the grid was one-half the error of the false-alarm outlooks, with the largest errors located well north of the Gulf. Although the sample of cases is quite small, the results suggest that the accuracy of the NGM lifted-index forecasts, which in turn influence the day 2 outlook, may also be partially dependent on the characteristics of the air mass along the Gulf coast during return-flow episodes.

7. Summary and discussion

Based on the findings of this study, the following guidelines were developed to assist forecasters in the interpretation and use of 48-h NMC model output in the cool-season prediction of anticyclone evolution, frontal movement into the Gulf, and return-flow development. These guidelines were designed for application over the Gulf of Mexico and the United States east of 105°W and were utilized extensively by the GUFMEX forecast team during the course of the field experiment.

1) Anticyclone location and pressure predictions

(a) The NGM and AVN display no significant bias in the location (movement) of anticyclones. The LFM has a pronounced tendency to move anticyclones eastward too rapidly.

(b) The NGM and AVN exhibit a small underforecast bias in the anticyclone central pressure, with the AVN showing the smallest mean error of less than 1 mb. The LFM weakens anticyclones much too rapidly with 48-h forecast errors averaging more than 5 mb too low.

(c) When surface pressures along the northwest Gulf coast are examined, the NGM and AVN again

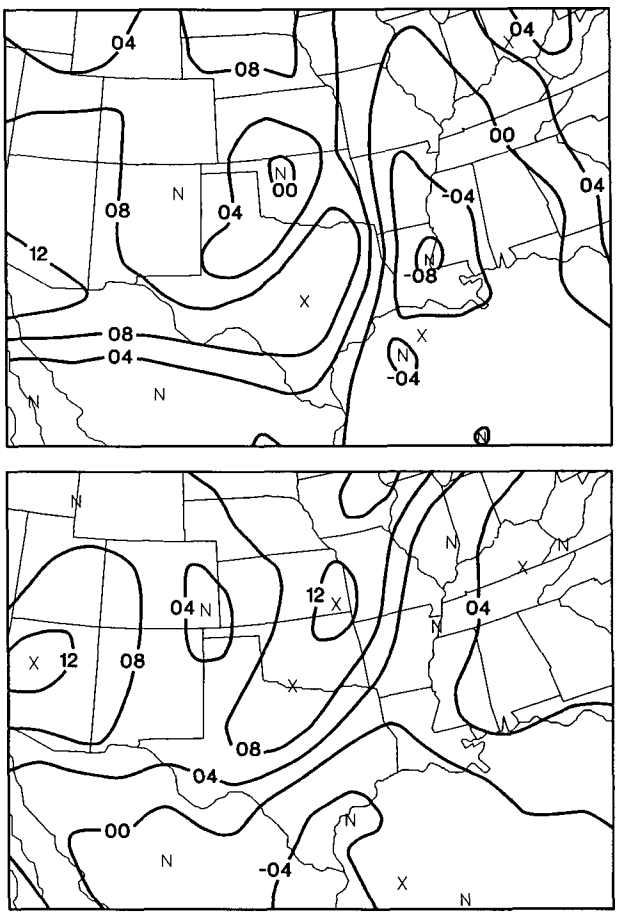

FIG. 14. NGM 48-h lifted-index forecast valid 0000 UTC 9 March 1988 (top), and verifying 00-h initial conditions (bottom). Note erroneous forecast of extreme instability over lower Mississippi Valley.

display a small underforecast bias, with the AVN having the smallest mean error of less than 1 mb. The LFM displays a persistent tendency to underforecast substantially pressures along the coast, with 48-h errors averaging nearly 8 mb too low.

2) Cold fronts moving into the Gulf

Cold fronts moving into the Gulf often are not accompanied by a well-defined pressure trough in the model output. The 1000–500-mb thickness pattern can assist in estimating the frontal location, especially when a strong thickness gradient exists on the cold-air side of the front. All models displayed moderate skill in the prediction of cold fronts across the Gulf.

3) Return-flow development

The NGM and AVN display reasonable skill in forecasting the onset of return flow at the coast. There was a slight tendency for these models to develop the return flow too slowly. The LFM typically overforecasts the occurrence of return flow. The onset may be predicted 24–36 h too early, and the LFM tends to open the Gulf from west to east too quickly.

It is important to note that even when a numerical weather prediction model exhibits systematic errors, information about these errors can be useful to forecasters. Knowledge that the LFM tends to develop return flow too quickly proved helpful during GUFMEX. Awareness of this bias provided forecasters with advance notice for each potential return-flow situation, and they were able to alert project scientists one to two days before the start of the actual return-flow events.

The results of this study also indicate that antecedent thermodynamic conditions along the Gulf coast can impact subsequent severe local storm potential, even up to two days in advance. This implies that there may be a finite amount of time, perhaps on the order of several days, necessary for the return-flow current to advect moisture inland and for the air mass to acquire the thermodynamic characteristics favorable for severe local storm development. The operational NGM and AVN models have been shown to have skill in predicting the surface-pressure (MSL) patterns associated with return-flow episodes up to 48 h in advance.

However, the accurate prediction of the surface-pressure field does not ensure that the actual moisture return and resultant thermodynamic profile will also be simulated properly. Janish and Lyons (1992) found that the NGM 48-h forecasts of return flow during GUFMEX were too dry, even though the kinematic structure of return-flow events was predicted fairly well in both timing and magnitude. Their results indicate the NGM model physics are unable to simulate airmass modification over the marine boundary layer properly, resulting in erroneous predictions of the depth and magnitude of the moist layer and the character of the low-level temperature profile. It is unclear at this time how the NGM low-level dry bias noted by Janish and Lyons (1992) during return-flow episodes is related to the lifted-index errors found in this study, since a dry boundary layer is usually indicative of a more stable air mass. Other aspects of the NGM model physics, such as convective parameterization and subsoil temperature and moisture, apparently play a role in predictions of excessive instability (Weiss 1987). Additional work is currently being done to examine NGM predictions during two return-flow–severe-weather cases that occurred in March 1990 and March 1991. Part of this research will investigate the relationship between the low-level moisture return and the airmass stability in the model atmosphere.

The largest lifted-index errors occurred just north of the Gulf. This is similar to the NGM quantitative precipitation forecast (QPF) errors reported by Junker and Hoke (1990), who found that during cool-season return-flow episodes the largest QPF errors were near the Gulf coast. They noted that the model forecast errors may result from a number of factors, ranging from the lack of observational data over the Gulf to limitations in model physics and data assimilation methods. It appears that the data void over the Gulf must have some impact on the accuracy of the initial conditions during return-flow situations. However, substantial errors in the NGM forecast lifted-index fields have been documented over all areas of the United States during summer when moisture is located well inland, implying that inaccurate model physics also contribute to forecast errors (Weiss 1987).

A more complete understanding of the model prediction errors could be obtained by conducting sensitivity tests to examine model response to varying inputs. Accordingly, plans are being developed by NSSL, NMC, the National Environmental Satellite, Data and Information Service (NESDIS) in Madison, Wisconsin, and NSSFC to incorporate special GUFMEX datasets, including soundings and satellite data over the Gulf, into the NGM and rerun the model during several GUFMEX cases. Two primary objectives of this research will be 1) improved understanding of the physical processes involved in return flow (such as vertical mixing, moisture advection, and leeside processes east of the Sierra Madre Oriental Mountains of eastern Mexico), and 2) aspects of numerical weather prediction (NWP) modeling and forecast applications. The performance of the NGM will be investigated with respect to factors such as the impact of special datasets, the impact of Mexican upper-air data (which are only occasionally available twice a day), the simulation of data at wind profiler resolution into the NWP job stream, the evolution of frontal boundaries over the Gulf and their interaction with the sea surface tem-

perature distribution, and insight into ways of separating the effects of high-resolution data from possible imperfections in the model physics and data-assimilation procedures. It is anticipated that this will provide considerable insight into the identification of factors contributing to the generation of some model forecast errors.

Acknowledgments. I am especially grateful to Dr. John Lewis of NSSL for his advice and encouragement during my participation in GUFMEX. Discussions with Drs. Charles Doswell (NSSL), Robert Maddox (NSSL), and Robert Merrill (CIMSS), and Messrs. Gary Grice and Stephen Rinard (NWS–Southern Region), were quite beneficial during the course of this research. I also thank Drs. Lewis, Maddox, and Preston Leftwich (NSSFC), Mr. Frederick Ostby (NSSFC), and the anonymous reviewers for their valuable comments and suggestions which improved the quality of the manuscript. Some of the figures were provided by Dr. Richard Livingston (NWS–Central Region), Ms. Joan Kimpel (NSSL), and Ms. Jan Lewis (NSSFC). This research was partially funded by the Texas Institute of Oceanography, the Institute for Naval Oceanography, the National Weather Service–Southern Region, and Texas A&M University, through the Cooperative Institute for Applied Meteorological Studies, Texas A&M.

REFERENCES

Alexander, G. D., and G. M. Young, 1990: The use of surface cyclone characteristics to determine systematic departures from mean Nested Grid Model forecast errors. *Nat. Wea. Digest,* **15,** 6–12.

Caplan, P. M., and G. H. White, 1989: Performance of NMC's medium range model. *Wea. Forecasting,* **4,** 391–400.

Colucci, S. J., and L. F. Bosart, 1979: Surface anticyclone behavior in NMC prediction models. *Mon. Wea. Rev.,* **107,** 377–394.

Crisp, C. A., and J. M. Lewis, 1992: Return flow in the Gulf of Mexico. Part I: A classificatory approach with a global historical perspective. *J. Appl. Meteor.,* **31,** 868–881.

Djurić, D., and M. S. Damiani, Jr., 1980: On the formation of the low-level jet over Texas. *Mon. Wea. Rev.,* **108,** 1854–1865.

——, and D. S. Ladwig, 1983: Southerly low-level jet in the winter cyclones of the southwestern Great Plains. *Mon. Wea. Rev.,* **111,** 2275–2281.

Donaldson, R. J., R. M. Dyer, and M. J. Kraus, 1975: An objective evaluator of techniques for predicting severe weather events. Preprints, *Ninth Conf. on Severe Local Storms,* Norman, Oklahoma, Amer. Meteor. Soc., 321–326.

Doswell, C. A., III, R. Davies-Jones, and D. L. Keller, 1990a: On summary measures of skill in rare event forecasting based on contingency tables. *Wea. Forecasting,* **5,** 576–585.

——, D. L. Keller, and S. J. Weiss, 1990b: An analysis of the temporal and spatial variation of tornado and severe thunderstorm watch verification. Preprints, *16th Conf. on Severe Local Storms,* Kananaskis Provincial Park, Alberta, Canada, Amer. Meteor. Soc., 294–299.

Fawcett, E. B., 1969: Systematic errors in operational baroclinic prognoses at the National Meteorological Center. *Mon. Wea. Rev.,* **97,** 670–682.

Galway, J. G., 1956: The lifted index as a predictor of latent instability. *Bull. Amer. Meteor. Soc.,* **37,** 528–529.

——, and A. D. Pearson, 1981: Winter tornado outbreaks. *Mon. Wea. Rev.,* **109,** 1072–1080.

Gerrity, J. F., 1977: The LFM model—1976: A documentation. NOAA Technical Memorandum NWS NMC-60, National Meteorological Center, Washington, D.C., 68 pp.

Grumm, R. H., and J. R. Gyakum, 1986: Systematic surface anticyclone errors in NMC's Limited-area Fine Mesh and Spectral models during the winter of 1981/82. *Mon. Wea. Rev.,* **114,** 2329–2343.

——, and A. L. Siebers, 1989a: Systematic surface cyclone errors in NMC's Nested Grid Model, November 1988 through January 1989. *Wea. Forecasting,* **4,** 246–252.

——, and ——, 1989b: Systematic surface anticyclone errors in Nested Grid Model run at NMC: December 1988–August 1989. *Wea. Forecasting,* **4,** 555–561.

Hawes, J. T., and S. J. Colucci, 1986: An examination of 500-mb cyclones and anticyclones in National Meteorological Center prediction models. *Mon. Wea. Rev.,* **114,** 2163–2175.

Henry, W. K., 1979: Some aspects of the fate of cold fronts in the Gulf of Mexico. *Mon. Wea. Rev.,* **107,** 1078–1082.

Hoke, J. E., N. A. Phillips, G. J. DiMego, J. J. Tuccillo, and J. G. Sela, 1989: The regional analysis and forecasting system of the National Meteorological Center. *Wea. Forecasting,* **4,** 323–334.

Janish, P. R., and S. W. Lyons, 1992: NGM performance during cold-air outbreaks and periods of return flow over the Gulf of Mexico with emphasis on moisture-field evolution. *J. Appl. Meteor.,* **31,** 995–1017.

Junker, N. W., 1985: Recognizing characteristic model errors and incorporating them into precipitation forecasts. Preprints, *Sixth Conf. on Hydrometeorology,* Indianapolis, Amer. Meteor. Soc., 270–276.

——, and J. E. Hoke, 1990: An examination of Nested Grid Model precipitation forecasts in the presence of moderate-to-strong low-level southerly inflow. *Wea. Forecasting,* **5,** 333–344.

——, ——, and R. H. Grumm, 1989: Performance of NMC's regional models. *Wea. Forecasting,* **4,** 368–390.

Kanamitsu, M., 1989: NMC's global spectral model and Global Data Assimilation System. *Wea. Forecasting,* **4,** 335–342.

Kelly, D. L., J. T. Schaefer, R. P. McNulty, C. A. Doswell III, and R. F. Abbey, Jr., 1978: An augmented tornado climatology. *Mon. Wea. Rev.,* **106,** 1172–1183.

——, ——, and C. A. Doswell III, 1985: Climatology of nontornadic severe thunderstorm events in the United States. *Mon. Wea. Rev.,* **113,** 1997–2014.

Lanicci, J. M., and T. T. Warner, 1991a: A synoptic climatology of the elevated mixed-layer inversion over the southern Great Plains in Spring. Part I: Structure, dynamics, and seasonal evolution. *Wea. Forecasting,* **6,** 181–197.

——, and ——, 1991b: A synoptic climatology of the elevated mixed-layer inversion over the southern Great Plains during spring. Part II: The life cycle of the lid. *Wea. Forecasting,* **6,** 198–213.

——, and ——, 1991c: A synoptic climatology of the elevated mixed-layer inversion over the southern Great Plains during Spring. Part III: Relationship to severe-storms climatology. *Wea. Forecasting,* **6,** 214–226.

Leary, C., 1971: Systematic errors in operational National Meteorological Center primitive-equation surface prognoses. *Mon. Wea. Rev.,* **99,** 409–413.

Leftwich, P. W., 1989: Verification of severe local storm forecasts issued by the National Severe Storms Forecast Center: 1988. NOAA Tech. Memo. NWS NSSFC-24, National Severe Storms Forecast Center, Kansas City, Missouri, 10 pp.

Lewis, J. M., C. M. Hayden, R. T. Merrill, and J. M. Schneider, 1989: GUFMEX: A study of return flow in the Gulf of Mexico. *Bull. Amer. Meteor. Soc.,* **70,** 24–29.

Mullen, S. L., and B. B. Smith, 1990: An analysis of sea-level cyclone errors in NMC's Nested Grid Model (NGM) during the 1987–88 winter season. *Wea. Forecasting,* **5,** 433–447.

Murphy, A. H., 1991: Probabilities, odds, and forecasts of rare events. *Wea. Forecasting.* **6,** 302–307.

——, and R. L. Winkler, 1971: Forecasters and probability forecasts: Some current problems. *Bull. Amer. Meteor. Soc.,* **52,** 239–247.

Newell, J. E., and D. G. Deaven, 1981: The LFM-II model—1980. NOAA Tech. Memo. NWS NMC 66, U.S. Dept. of Commerce, Washington, D.C., 20 pp.

Newton, C. W., 1963: Dynamics of severe convective storms. *Severe Local Storms,* Meteorol. Monograph 5, **27,** Amer. Meteor. Soc., Boston, 33–58.

——, 1967: Severe convective storms. *Advances in Geophysics, Vol. 12,* Academic Press, 257–303.

Phillips, N. A., 1979: The Nested Grid Model. NOAA Technical Report NWS-22, National Oceanic and Atmospheric Administration, Silver Spring, Maryland, 80 pp.

Saucier, W. J., 1955: *Principles of Meteorological Analysis.* University of Chicago Press, 438 pp.

Schecter, R., 1984: An error analysis of LFM-II forecasts during the 1982–1983 winter season. *Bull. Amer. Meteor. Soc.,* **65,** 1073–1080.

Sela, J. G., 1980: Spectral modeling at the National Meteorological Center. *Mon. Wea. Rev.,* **108,** 1279–1292.

——, 1988: The new NMC operational spectral model. Preprints, *Eighth Conf. on Numerical Weather Prediction,* Baltimore, Amer. Meteor. Soc., 312–313.

Showalter, A. K., 1953: A stability index for thunderstorm forecasting. *Bull. Amer. Meteor. Soc.,* **34,** 250–252.

Shuman, F. G., and J. B. Hovermale, 1968: An operational six-layer primitive equation model. *J. Appl. Meteor.,* **7,** 525–547.

Silberberg, S. R., and L. F. Bosart, 1982: An analysis of systematic cyclone errors in the NMC LFM-II model during the 1978–79 cool season. *Mon. Wea. Rev.,* **110,** 254–271.

United States Weather Bureau, 1956: Forecasting severe thunderstorms and tornadoes. *Forecasting Guide No. 1,* U.S. Weather Bureau, Washington, D.C., 34 pp.

Weiss, S. J., 1987: An assessment of the NGM four-layer lifted index prognoses of extreme instability. *Nat. Wea. Digest,* **12,** 21–31.